PHYSICS AND CHEMISTRY OF SOLID STATE
V.21, No.2 (2020) pp. 272-278

Vasyl Stefanyk Precarpathian National University

ФІЗИКА І ХІМІЯ ТВЕРДОГО ТІЛА
Т. 21, № 2 (2020) С. 272-278

DOI: 10.15330/pcss.21.2.272-278

UDK 546.882 ISSN 1729-4428

L. Romaka[1], Yu. Stadnyk[1], V.V. Romaka[2,3], A. Horpenyuk[2]

Phase Equilibria in Ho-Fe-Sn Ternary System at 670 K

[1]*Ivan Franko L'viv National University, L'viv, Ukraine, lyubov.romaka@gmail.com*
[2]*Lviv Polytechnic National University, Lviv, Ukraine, lygecka@i.ua*
[3]*Institute for Solid State Research, IFW-Dresden, Dresden, Germany, vromaka@gmail.com*

Interaction between the components in the Ho-Fe-Sn ternary system was studied using X-ray diffractometry, metallography and electron microprobe analysis. Isothermal section of the phase diagram was constructed at 670 K over the whole concentration range. Component interaction in the Ho-Fe-Sn system at 670 K results in the existence of one ternary compound $HoFe_6Sn_6$ which crystallizes in the YCo_6Ge_6 structure type (space group *P*6/*mmm*, a = 0.53797(2), c = 0.44446(2) nm). The interstitial-type solid solution $HoFe_xSn_2$ (up to 8 at.% Fe) based on the $HoSn_2$ ($ZrSi_2$-type structure) binary compound was found. Solubility of Sn in the $HoFe_2$ binary ($MgCu_2$ structure type) extends up to 5 at. %.

Keywords: intermetallics; stannides; phase diagrams; crystal structure; X-ray diffraction.

Received 22 January 2020; Accepted 15 June 2020.

Introduction

Intermetallic phases containing rare earths (R), iron and *p*-elements display interesting physical properties. According to the magnetic data of the ternary stannides the $Pr_6Fe_{13}Sn$, $Nd_6Fe_{13}Sn$ and $Sm_6Fe_{13}Sn$ compounds ($Pr_6Fe_{13}Ge$ structure type) are characterized by high temperatures of the magnetic ordering [1, 2]. Magnetic properties of the RFe_6Sn_6 compounds (R = Y, Gd, Tb, Dy, Ho, Er, Tm) have been studied by magnetization measurements and Mössbauer spectroscopy. These results confirm antiferromagnetic ordering of the compounds below a Néel point of ~ 400 K [3]. Neutron diffraction data of the RFe_6Sn_6 stannides showed the different magnetic ordering of Fe and rare earth sublattices performed at different temperatures [4].

The physical (magnetic, electric, mechanic) properties of the intermetallics in many cases are strongly dependent on the synthesis, microstructure of the alloys, heat treatments, the stability, homogeneity domains, and structural disordering of the intermediate phases. In this context the investigation of the R–Fe–Sn ternary systems at selected temperatures is very important, in order to provide valuable information of the sample preparation method, stability, composition and crystal structure peculiarity of the ternary compounds. The R-Fe-Sn ternary phase equilibrium diagrams have been constructed for Y, Pr, Nd, Sm, Gd, Dy and Er [2, 5-9], the preliminary investigations were carried out also for La-Fe-Sn and Lu-Fe-Sn systems [10]. Study of the Er-Fe-Sn system at 670 and 770 K [9] showed an influence of the temperature on stability of the ternary phase at high Sn content. For other rare earth metals only individual alloys were studied to identify isostructural compounds for structural and physical property investigations. A review of the literature shows that the most of the R-Fe-Sn systems is characterized by existence of the ternary compounds with RFe_6Sn_6 stoichiometry. These compounds crystallize in the hexagonal YCo_6Ge_6-type or in the various superstructures [5-9]. In the Dy-Fe-Sn system (1070 K) the $DyFe_6Sn_6$ compound crystallizes in the YFe_6Sn_6-type structure (space group *Cmcm*), while $Dy_xFe_6Sn_6$ (x = 0.32 and 0.5) is isotype to the partially-ordered $SmMn_6Sn_6$-type (space group *P*6/*mmm*) [8]. At other annealing temperatures $DyFe_6Sn_6$ compound crystallizes in the $DyFe_6Sn_6$ structure type (1123 K) [11] or $TbFe_6Sn_6$-type (1273 K) with orthorhombic unit cell [12].

Unlike the R-Fe-Sn systems, where R is the rare earth metals of the Cerium subgroup, only one ternary compound with a stoichiometry of 1: 6: 6 is formed in the investigated {Y, Gd, Dy}-Fe-Sn systems [5, 8]. The

study of the Er-Fe-Sn system at annealing temperature 670 K [9], in addition to the $ErFe_6Sn_6$ stannide, revealed the formation of another compound $Er_5Fe_6Sn_{18}$ with a cubic structure of the $Tb_5Rh_6Sn_{18}$-type. A new ternary compound in the Lu-Fe-Sn system with a high Sn content ~$Lu_4Fe_6Sn_{19}$, which the authors identified as a cubic phase with a lattice parameter a = 1.3537 nm, was reported in the Ref. [10]. Further structural studies have demonstrated that the ~$Lu_4Fe_6Sn_{19}$ phase corresponds to the $Lu_5Fe_6Sn_{18}$ compound with the $Tb_5Rh_6Sn_{18}$ type structure (a = 1.3235 nm) [13] and is isostructural to the $Er_5Fe_6Sn_{18}$ compound [9].

The subject of the present paper consists of the complete investigation of the Ho-Fe-Sn phase equilibrium diagram at 670 K by X-ray powder diffraction and electron microprobe analysis (EPMA).

I. Experimental details

The samples with the weight of 1g were prepared by a direct twofold arc melting of the constituent elements (holmium, purity of 99.9 wt.%; iron, purity of 99.99 wt.%; and tin, purity of 99.999 wt.%) under high purity Ti-gettered argon atmosphere on a water-cooled copper crucible. After melting the overall weight losses of the alloys were generally less than 1 wt. %. The pieces of the as-cast buttons were annealed for one month at 670 K in evacuated silica tubes. The temperature of annealing was chosen taking into account the low melting temperature of Sn (232^0C) and of the Ho-Sn binaries at high Sn content [14]. The ampoules with annealed ingots were removed from the furnace and quenched in cold water.

Phase analysis was performed using X-ray powder diffraction patterns of the synthesized samples annealed at 670 K (diffractometer DRON-4.0, Fe $K\alpha$ radiation). The experimental diffraction intensities were compared with reference powder patterns of pure elements, binary and known ternary phases. The elemental and phase compositions of the prepared samples were examined by scanning electron microscopy (SEM) using REMMA-102-02 scanning microscope. Quantitative electron probe microanalysis (EPMA) of the alloys was carried out by using an energy-dispersive X-ray analyser with the pure elements as standards (an acceleration voltage was 20 kV; *K*- and *L*-lines were used). The data for the crystal structure refinements were collected at room temperature using STOE STADI P diffractometer (graphite monochromator, Cu $K\alpha_1$ radiation). Calculations of the crystallographic parameters were performed with the WinCSD and FullProof suite program packages [15, 16].

II. Results and discussion

The binary boundary Ho-Fe, Ho-Sn and Fe-Sn systems, which delimit Ho-Fe-Sn system, have been investigated earlier, their phase diagrams and crystallographic characteristics of the binary compounds are reported in the literature [14, 17-19]. In the Fe-Sn system we confirmed the existence of the FeSn (CoSn-type) and $FeSn_2$ ($CuAl_2$-type) binaries at 670 K in agreement with Refs. [17, 18], other two phases Fe_3Sn and Fe_3Sn_2 formed above 870 K were not observed at investigated temperature.

The Ho-Sn state diagrams used for our investigation were taken from Refs. [14, 19]. We have synthesized all the samples in the Ho-Sn system with the stoichiometry corresponding to the literature data. The performed phase analysis confirmed the formation of the Ho_5Sn_3 (Mn_5Si_3-type), Ho_5Sn_4 (Sm_5Ge_4-type), $Ho_{11}Sn_{10}$ ($Ho_{11}Ge_{10}$-type), $HoSn_2$ ($ZrSi_2$-type), Ho_2Sn_5 (Er_2Ge_5-type) and $HoSn_3$ ($GdSn_{2.75}$-type) binaries. The Ho_4Sn_5 [19] and Ho_3Sn_7 [20] binaries were not identified at the annealing temperature, corresponding samples contain two phases $Ho_{11}Sn_{10}$, $HoSn_2$ and Ho_2Sn_5, $HoSn_2$, respectively.

According to the references [17, 21] the Ho-Fe binary phase diagram was investigated above 970 K, four binary compounds Ho_2Fe_{17} (Th_2Ni_{17}-type), Ho_6Fe_{23} (Th_6Mn_{23}-type), $HoFe_3$ ($PuNi_3$-type) and $HoFe_2$ ($MgCu_2$-

Table 1

Crystallographic characteristics of the Ho-Fe, Ho-Sn and Fe-Sn binary compounds

Compound	Structure type	Space group	Lattice parameters, nm			Ref.
			a	*b*	*c*	
Ho_2Fe_{17}	Th_2Ni_{17}	$P6_3/mmc$	0.8433(4)	-	0.8306(5)	this work
Ho_6Fe_{23}	Th_6Mn_{23}	Fm-3m	1.2027(4)	-	-	this work
$HoFe_3$	$PuNi_3$	R-3m	0.5109(3)	-	2.4477(4)	this work
$HoFe_2$	$MgCu_2$	Fd-3m	0.7290(2)	-	-	this work
Ho_5Sn_3	Mn_5Si_3	$P6_3/mcm$	0.8845(3)	-	0.6446(3)	this work
Ho_5Sn_4	Sm_5Ge_4	$Pnma$	0.7963(3)	1.5302(5)	0.8053(2)	this work
$Ho_{11}Sn_{10}$	$Ho_{11}Ge_{10}$	$I4/mmm$	1.1526		1.6768	[22]
$HoSn_2$	$ZrSi_2$	$Cmcm$	0.4381(2)	1.6190(5)	0.4288(2)	this work
Ho_2Sn_5	Er_2Ge_5	$Pmmn$	0.4307(2)	0.4387(3)	1.8907(5)	this work
$HoSn_3$	$GdSn_{2.75}$	$Amm2$	0.4335	0.4373	2.1757	[14]
FeSn	CoSn	$P6/mmm$	0.5300		0.4450	[23]
$FeSn_2$	$CuAl_2$	$I4/mcm$	0.6531(3)		0.5326(3)	this work

Table 2

EPMA and crystallographic data for selected Ho-Fe-Sn alloys annealed at 670 K

Nominal composition	Phase	Structure type	Lattice parameters, nm			EPMA data, at %		
			a	*b*	*c*	Ho	Fe	Sn
$Ho_{33}Fe_{60}Sn_7$	$HoFe_xSn_{2-x}$	$MgCu_2$	0.7316(6)					
	$HoFe_3$	$PuNi_3$	0.5091(3)		2.4479(6)			
	Ho_5Sn_3	Mn_5Si_3	0.8841(2)		0.6452(3)			
$Ho_{30}Fe_{60}Sn_{10}$	Ho_6Fe_{23}	Th_6Mn_{23}	1.2043(5)					
	$HoFe_3$	$PuNi_3$	0.5089(4)		2.4482(6)			
	Ho_5Sn_3	Mn_5Si_3	0.8846(3)		0.6453(4)	62.37		37.63
$Ho_{55}Fe_{30}Sn_{15}$	$HoFe_2$	$MgCu_2$	0.7296(4)			33.11	66.89	
	Ho_5Sn_3	Mn_5Si_3	0.8848(4)		0.6456(3)	62.37		37.63
	(Ho)	Mg	0.3579(3)		0.5596(4)	99.98		
$Ho_{20}Fe_{60}Sn_{20}$	$Ho_{11}Sn_{10}$	$Ho_{11}Ge_{10}$	1.1526(5)		1.6768(6)			
	(Fe)	W	0.2873(2)					
$Ho_{15}Fe_{55}Sn_{30}$	(Fe)	W	0.2872(3)				99.99	
	$HoFe_xSn_2$	$ZrSi_2$	0.4403(3)	1.6221(6)	0.4338(5)	30.29	7.63	62.08
$Ho_{50}Fe_{10}Sn_{40}$	$Ho_{11}Sn_{10}$	$Ho_{11}Ge_{10}$	1.1525(5)		1.6770(7)			
	Ho_5Sn_4	Sm_5Ge_4	0.7963(3)	1.5302(5)	0.8054(3)			
	(Fe)	W	0.2873(3)					
$Ho_{20}Fe_{40}Sn_{40}$	$HoFe_xSn_2$	$ZrSi_2$	0.4403(3)	1.6222(5)	0.4337(4)	29.59	7.76	62.65
	(Fe)	W	0.2874(2)				99.97	
$Ho_{30}Fe_{25}Sn_{45}$	$HoFe_xSn_2$	$ZrSi_2$	0.4402(4)	1.6223(5)	0.4336(4)	30.46	7.77	61.77
	$Ho_{11}Sn_{10}$	$Ho_{11}Ge_{10}$	1.1525(5)		1.6767(7)	52.48		47.52
	(Fe)	W	0.2873(3)				99.98	
$Ho_5Fe_{45}Sn_{50}$	FeSn	CoSn	0.5298(3)		0.4446(3)			
	$HoFe_6Sn_6$	YCo_6Ge_6	0.5380(4)		0.4445(4)			
	$FeSn_2$	$CuAl_2$	0.6532(3)		0.5318(3)			
$Ho_{20}Fe_{30}Sn_{50}$	$HoFe_xSn_2$	$ZrSi_2$	0.4404(4)	1.6224(5)	0.4335(3)	29.78	8.02	62.20
	$HoFe_6Sn_6$	YCo_6Ge_6	0.5379(4)		0.4444(4)	6.09	47.08	46.83
	(Fe)	W	0.2872(4)				100.0	
$Ho_{15}Fe_{25}Sn_{60}$	$HoFe_xSn_2$	$ZrSi_2$	0.4401(4)	1.6221(6)	0.4338(4)			
	$FeSn_2$	$CuAl_2$	0.6531(4)		0.5319(3)			
	$HoFe_6Sn_6$	YCo_6Ge_6	0.5380(5)		0.4445(4)			
$Ho_{15}Fe_{20}Sn_{65}$	$FeSn_2$	$CuAl_2$	0.6533(4)		0.5321(3)		32.88	67.12
	$HoFe_xSn_2$	$ZrSi_2$	0.4406(3)	1.6207(6)	0.4309(4)	30.24	7.39	62.20
$Ho_{27}Fe_{13}Sn_{60}$	$HoFe_xSn_2$	$ZrSi_2$	0.4401(3)	1.6222(6)	0.4335(3)	30.84	6.79	62.47
	$HoFe_6Sn_6$	YCo_6Ge_6	0.5380(4)		0.4444(4)	6.23	47.49	46.28
$Ho_{20}Fe_{13}Sn_{67}$	$FeSn_2$	$CuAl_2$	0.6532(4)		0.5323(4)			
	$HoFe_xSn_2$	$ZrSi_2$	0.4405(3)	1.6223(6)	0.4336(4)			
	Ho_2Sn_5	Er_2Ge_5	0.4305(3)	0.4392(4)	1.8925(5)			

type) were found to exist. To check the formation of the reported binary compounds under our conditions, the samples of the corresponding compositions were synthesized and annealed at 670 K. Performed phase analysis showed the presence of the Ho_2Fe_{17} (Th_2Ni_{17}-type), Ho_6Fe_{23} (Th_6Mn_{23}-type), $HoFe_3$ ($PuNi_3$-type), and $HoFe_2$ ($MgCu_2$-type) phases at investigated temperature. Crystallographic characteristics of the binary compounds of the Ho-Fe, Ho-Sn and Fe-Sn systems are presented in Table 1.

Solubility of Sn in the $HoFe_2$ ($MgCu_2$-type) binary extends up to 5 at. % (a = 0.7290(2) nm for $HoFe_2$ and a = 0.73168(5) nm for $Ho_{33}Fe_{62}Sn_5$ sample). The solubility of Sn in other compounds of the Ho-Fe system, as well as of the third component in the binary compounds of the Fe-Sn and Ho-Sn (except $HoSn_2$ binary) systems does not exceed 1-2 at. %.

To establish the phase relations in the Ho-Fe-Sn ternary system prepared binary and ternary alloys were examined by XRPD and EPM analyses. Based on the obtained results the isothermal section of the Ho-Fe-Sn system was constructed at 670 K over the whole concentration range (Fig. 1). The phase composition and EPMA data for the selected alloys are given in Table 2, electron microphotographs of some alloys are shown in Fig. 2.

In course of our study the interstitial-type solid solution $HoFe_xSn_2$ (up to 8 at. % Fe) based on the $HoSn_2$ ($ZrSi_2$-type, space group *Cmcm*) binary compound was observed similarly to [24, 25]. The limit composition of this solid solution was estimated from the systematic analysis of the cell parameters (a = 0.4403(3), b = 1.6223(5), c = 0.4337(4) nm for $Ho_{31}Fe_8Sn_{61}$ sample) and by the results of electron microprobe analysis ($Ho_{30.29}Fe_{7.63}Sn_{62.08}$). The volume of the unit-cell increases with Fe content (V=0.3041 nm^3 for $HoSn_2$,

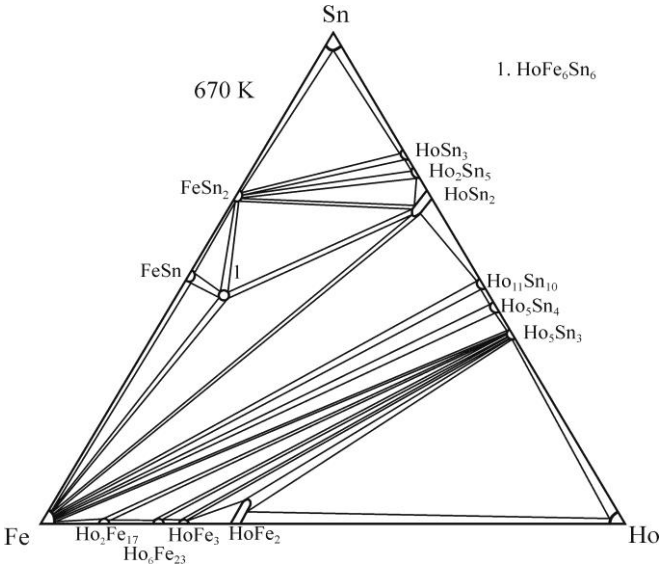

Fig. 1. Isothermal section of the Ho-Fe-Sn system at 670 K

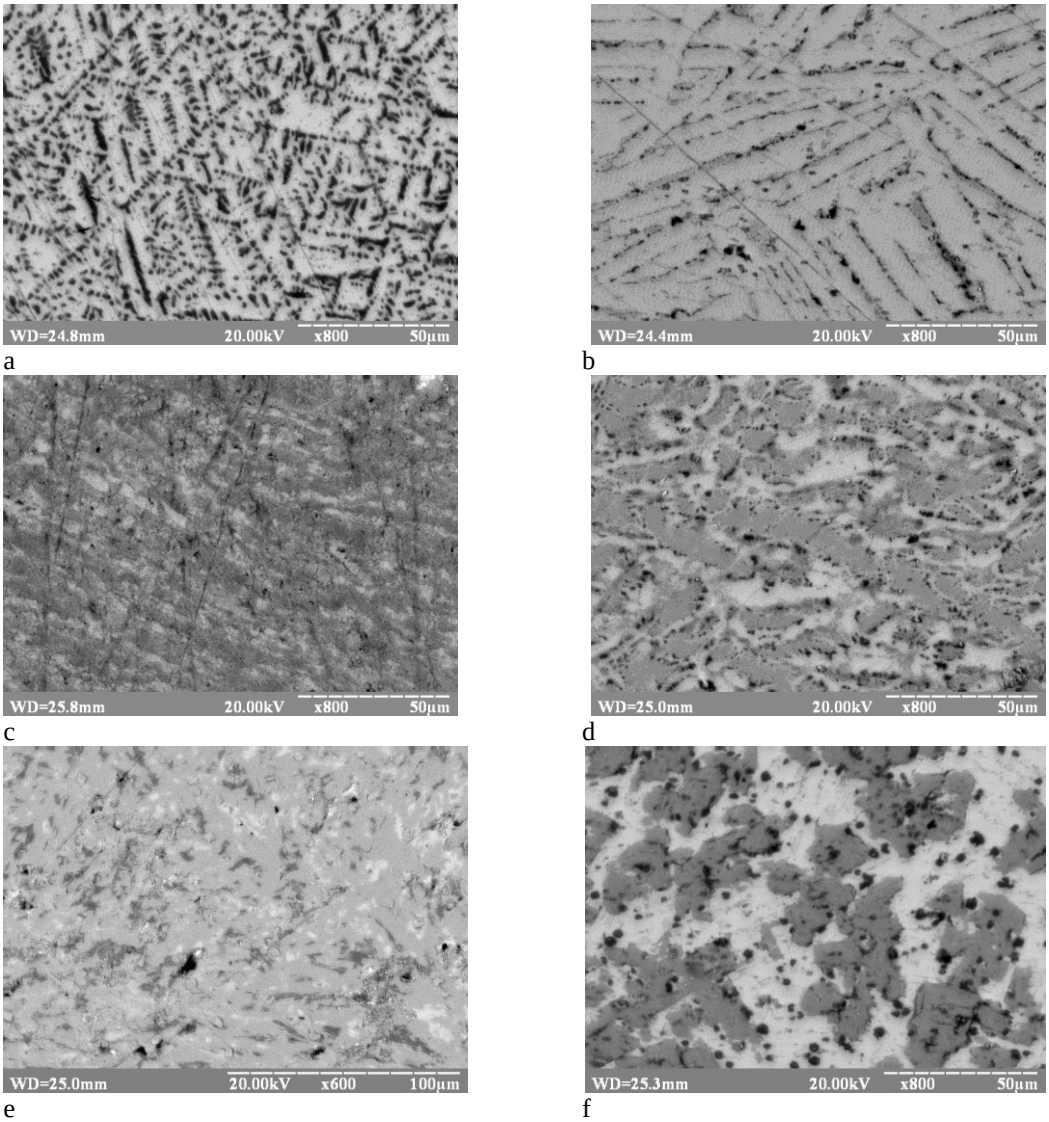

Fig. 2. Electron microphotographs of the Ho-Fe-Sn alloys (670 K): *a*) $Ho_{20}Fe_{40}Sn_{40}$ ($HoFe_xSn_2$ – light phase, (Fe) – black phase); *b*) $Ho_{27}Fe_{13}Sn_{60}$ ($HoFe_xSn_2$ ($Ho_{31,6}Fe_{5,3}Sn_{63,1}$) – light phase, $HoFe_6Sn_6$ – dark phase); *c*) $Ho_{20}Fe_{13}Sn_{67}$ ($HoFe_xSn_2$ – grey phase, $FeSn_2$ – dark phase, Ho_2Sn_5 – light phase); *d*) $Ho_{20}Fe_{30}Sn_{50}$ ($HoFe_6Sn_6$ – grey phase, $HoFe_xSn_2$ – light phase, (Fe) – dark phase); e) $Ho_{15}Fe_{25}Sn_{60}$ ($HoFe_xSn_2$ – light phase, $HoFe_6Sn_6$ – grey phase, $FeSn_2$ – dark phase); f) $Ho_{30}Fe_{25}Sn_{45}$ ($HoFe_xSn_2$ – light phase, $Ho_{11}Sn_{10}$ – grey phase, (Fe) – dark phase).

$V = 0.3098$ nm^3 for $Ho_{31}Fe_8Sn_{61}$) confirming the insertion-type of the solid solution. The sample $Ho_{27}Fe_{13}Sn_{60}$ contains two phases in equilibrium - $HoFe_xSn_2$ and $HoFe_6Sn_6$ (Fig. 2,b).

According to performed X-ray phase and electron microprobe analyses the phase relations in the Ho-Fe-Sn system at 670 K are characterized by the formation of one ternary compound $HoFe_6Sn_6$. Performed crystal structure calculations showed that the $HoFe_6Sn_6$ compound belongs to the hexagonal YCo_6Ge_6-type (space group *P*6/*mmm*, $a = 0.53797(2)$, $c = 0.44446(2)$ nm) [26] under used in our work conditions. Refined atomic parameters for the $HoFe_6Sn_6$ stannide are given in Table 3. According to the performed calculations, there is an incomplete filling of positions 1*a* for Ho atoms and 2*e* for Sn2 atoms (Table 3). The obtained result is consistent with the data of Ref. [26].

YCo_6Ge_6 structure type (space group *P*6/*mmm*) is derivative from binary CoSn structure type (space group *P*6/*mmm*), which forms by insertion of the rare earth atoms into hexagonal voids of the CoSn structure [26]. Structural studies showed that the RFe_6Sn_6 stannides with YCo_6Ge_6 structure type are characterized by incomplete occupancy of the crystallographic positions 1*a* for R atoms and 2*e* for Sn2 atoms [9, 10, 26], which may be due to the small value of the parameter *c*. An increase of the parameter *c* leads to the structure ordering and realization of the series YFe_6Sn_6, $TbFe_6Sn_6$, $DyFe_6Sn_6$, $HoFe_6Sn_6$, $ErFe_6Sn_6$ structure types with orthorhombic unit cell [27]. According to Ref. [11] $HoFe_6Sn_6$ compound crystallizes in the $HoFe_6Sn_6$ structure type (space group *Immm*) at annealing temperature 1123 K, while using the lower annealing temperature (670 K or 870 K) leads to the implementation of the YCo_6Ge_6 structure type with partial filling of the crystallographic sites for Ho and Sn2 atoms.

Structure of the $HoFe_6Sn_6$ compound (YCo_6Ge_6-type) contains the structural fragments of the $CaCu_5$-type. The main structural fragment is six capped hexagonal prism (Fig. 3). Similar fragments are observed and in the structure of the Ho_2Fe_{17} binary compound with the Th_2Ni_{17} structure type (space group *P*6$_3$/*mmc*).

As it was reported in Ref. [9] a formation of the $Er_5Fe_6Sn_{18}$ compound with the cubic $Tb_5Rh_6Sn_{18}$ structure type was found in the Er-Fe-Sn system at 670 K. The existence of an isostructural compound has also been established for Lu [13]. Our attempt to find analogous phase in the Ho-Fe-Sn system was unsuccessful. Phase analysis and EPMA data of the

Table 3

Atomic coordinates and isotropic displacement parameters for $HoFe_6Sn_6$ compound
(space group *P*6/*mmm*, $a = 0.53797(2)$, $c = 0.44446(2)$ nm, $R_p = 0.0569$, $R_{wp} = 0.0741$, $R_{Bragg} = 0.0668$)

Atom	Wyckoff position	*x*/*a*	*y*/*b*	*z*/*c*	$B_{iso}\cdot10^2$ (nm^2)	Occupation
Ho	1*a*	0	0	0	0.60(1)	0.4(4)
Fe	3*g*	1/2	0	1/2	0.60(1)	1
Sn1	2*c*	1/3	2/3	0	0.59(8)	1
Sn2	2*e*	0	0	0.3329(8)	0.58(1)	0.47(3)

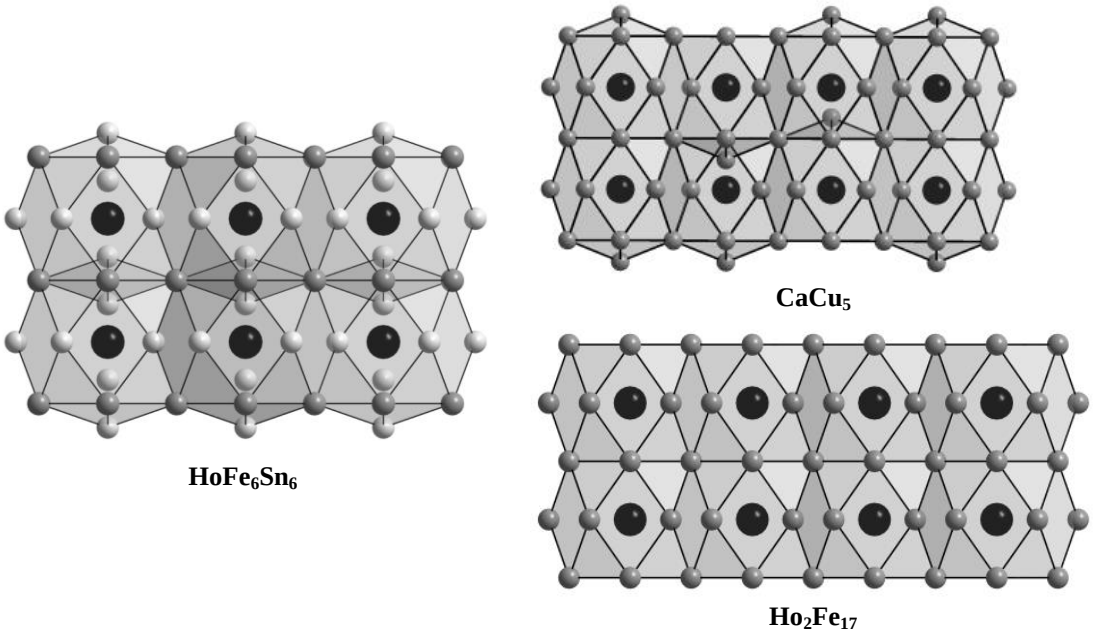

Fig. 3. $HoFe_6Sn_6$ and Ho_2Fe_{17} compounds derivative from $CaCu_5$ structure type.

$Ho_{15}Fe_{25}Sn_{60}$ sample showed three phases in equilibrium - $HoFe_xSn_2$, $FeSn_2$, and $HoFe_6Sn_6$ (Fig. 1, Fig. 2, e). The phase analysis of the samples with higher Sn indicated that the corresponding samples belong to the two- or three-phase fields: $Ho_{15}Fe_{20}Sn_{65}$ -$FeSn_2$ + $HoSn_2$; $Ho_{20}Fe_{13}Sn_{67}$ -$HoFe_xSn_2$ +$FeSn_2$ + Ho_2Sn_5 (Fig. 2, c).

Conclusions

An analysis of carried out investigations showed that interaction of holmium with iron and tin at annealing temperature 670 K results in the formation of one ternary compound $HoFe_6Sn_6$ with the YCo_6Ge_6 structure type. It should be noticed that the reduced number of the ternary phases in the Ho-Fe-Sn systems does not differ from the studied previously related {Y, Gd, Dy}-Fe-Sn and Er-Fe-Sn systems at 770 K. For the R–Fe–Sn systems, where R are heavy rare earth elements, the existence of the ternary phases, RFe_6Sn_6, crystallizing in the hexagonal YCo_6Ge_6-type (*P*6/*mmm* space group), or various superstructures of the YCo_6Ge_6-type was found. A formation of interstitial-type solid solutions RFe_xSn_2 based on the RSn_2 binary compounds with $ZrSi_2$ structure type was observed in the all studied R-Fe-Sn system where R is a rare earth of Yttrium group.

Acknowledgements

We would like to acknowledge financial support of the Ministry of Education and Science of Ukraine under Grant No. 0118U003609.

Romaka L. - Ph.D., Senior Scientist;
Stadnyk Yu. - Ph.D., Senior Scientist;
Romaka V. - D.Sc., Assoc. Professor;
Horpenyuk A. - Ph.D., associate professor.

[1] F. Weitzer, A. Leithe-Jasper, P. Rogl, K. Hiebl, H. Noel, G. Wiesinger, W. Steiner, Solid State Chem. 104, 368 (1993) (https://doi.org/10.1006/jssc.1993.1172).
[2] J. Stepien-Damm, E. Galdeska, O.I. Bodak, B.D. Belan, J. Alloys Compd. 298, 26 (2000). (https://doi.org/10.1016/S0925-8388(99)00626-X).
[3] X.-L. Rao, J.M.D. Coey, J. Appl. Phys. 81, 5181 (1997) (https://doi.org/10.1063/1.365164).
[4] J. M. Cadogan, D. H. Ryan, J. Alloys Compd. 326, 166 (2001) (https://doi.org/10.1016/S0925-8388(01)01242-7).
[5] Ya. Mudryk, L. Romaka, Yu. Stadnyk, O. Bodak, D. Fruchart, J. Alloys Compd. 383, 162 (2004) (https://doi.org/10.1016/j.jallcom.2004.04.040).
[6] J. Stepien-Damm, O.I. Bodak, B.D. Belan, E. Galdeska, J. Alloys Compd. 298, 169 (2000) (https://doi.org/10.1016/S0925-8388(99)00625-8).
[7] P. Salamakha, P. Demchenko, O. Sologub, O. Bodak, J. Stepien-Damm, Polish J. Chem. 71, 305 (1997).
[8] L.C.J. Pereira, D.P. Rojas, J.C. Waerenborgh, J. Alloys Compd. 396, 108 (2005) (https://doi.org/10.1016/j.jallcom.2004.11.061).
[9] L. Romaka, V.V. Romaka, P. Demchenko, R. Serkiz, J. Alloys Compd. 507, 67 (2010) (https://doi.org/10.1016/j.jallcom.2010.07.137).
[10] R.V. Skolozdra, in: K.A. Gschneidner, Jr. and L. Eyring (Eds.), Handbook on the Physics and Chemistry of Rare Earths, 24, (1997).
[11] B. Chafik, E. Idrissi, G. Venturini, B. Malaman, Mater. Res. Bull. 26, 1331 (1991) (https://doi.org/10.1016/0025-5408(91)90149-G).
[12] O.Y. Oleksyn, H. Böhm, Z. Kristallogr. 213, 270 (1998) (https://doi.org/10.1524/zkri.1998.213.5.270).
[13] I. Shcherba, L. Romaka, A. Skoblik, B. Kuzel, H. Noga, L. Bekenov, Yu. Stadnyk, P. Demchenko, A. Horyn, Acta Phys. Pol. A 136, 158 (2019) (https://10.12693/APhysPolA.136.158).
[14] A. Palenzona, P. Manfrinetti, J. Alloys Compd. 201, 43 (1993) (https://doi.org/10.1016/0925-8388(93)90859-L).
[15] L. Akselrud, Yu. Grin, WinCSD: software package for crystallographic calculations (Version 4), J. Appl. Crystallogr. 47, 803 (2014) (https://doi.org/10.1107/S1600576714001058).
[16] T. Roisnel, J. Rodriguez-Carvajal, Mater. Sci. Forum, Proc. EPDIC7 378-381, 118 (2001) (https://doi.org/10.4028/www.scientific.net/MSF.378-381.118).
[17] T.B. Massalski, in: Binary Alloy Phase Diagr., ASM (Metals Park, Ohio, 1990).
[18] P. Villars, L.D. Calvert, in: Pearson's Handbook of Crystallographic Data for Intermetallic Phases, ASM (Metals Park, OH, 1991).
[19] M.V. Bulanova, V.N. Eremenko, V.M. Petjukh, V.R. Sidorko, J. Phase Equil. 19, 136 (1998) (https://doi.org/10.1361/105497198770342599).
[20] K. Meier, L. Vasylechko, R. Cardoso-Gil, U. Burkardt, W. Schnelle, M. Schmidt, Yu. Grin, U. Schwarz, Z. Anorgan, Allg. Chem. 636(9-10), 1695 (2010).
[21] G.J. Roe, T.J. O'Keefe, Metallurg. Transact. 1, 2565 (1970).
[22] L. Romaka, I. Romaniv, V.V. Romaka, M. Konyk, A. Horyn, Yu. Stadnyk, Phys. chem. solid state 19(2), 139 (2018) (https://doi.org/10.15330/pcss.19.2.139-146).
[23] H. Noel, A.P. Goncalves, Intermetallics 9, 473 (2001) (https://doi.org/10.1016/S0966-9795(01)00026-7).

[24] G. Venturini, M. Francois, B. Malaman, B. Roques, J. Less-Common Met. 160, 215 (1990) (https://doi.org/10.1016/0022-5088(90)90382-T).
[25] M. Francois, G. Venturini, B. Malaman, B. Roques, J. less-Common Met. 160, 197 (1990) (https://doi.org/10.1016/0022-5088(90)90381-S).
[26] O.E. Koretskaya, R.V. Skolozdra, Inorg. Mater. 22, 690 (1986).
[27] G. Venturini, H. Ihou-Mouko, C. Lefevre, S. Lidin, B. Malaman, T. Mazet, J. Tobola, A. Verniere, Chem. Met. Alloys. 1, 24 (2008).

Л. Ромака[1], Ю. Стадник[1], В.В. Ромака[2,3], А. Горпенюк[2]

Фазові рівноваги в потрійній системі Ho-Fe-Sn при 670 K

[1]*Львівський національний університет ім. І.Франка, Львів, Україна, lyubov.romaka@gmail.com*
[2]*Національний університет "Львівська політехніка", Львів, Україна, lygecka@i.ua*
[3]*Інститут дослідження твердого тіла, Дрезден, Німеччина, vromaka@gmail.com*

Взаємодія компонентів у потрійній системі Ho-Fe-Sn досліджена методами рентгенівської дифракції, металографічного і рентгеноспектрального аналізів. Ізотермічний переріз діаграми стану системи побудований за температури 670 K в повному інтервалі концентрацій. Взаємодія компонентів у системі Ho-Fe-Sn при 670 K характеризується існуванням однієї тернарної сполуки $HoFe_6Sn_6$ (структурний тип YCo_6Ge_6, просторова група *P*6/*mmm*, *a* = 0,53797(2), *c* = 0,44446(2) нм). На основі бінарної сполуки $HoSn_2$ (структурний тип $ZrSi_2$) встановлено утворення твердого розчину включення $HoFe_xSn_2$ (до вмісту 8 ат.% Fe). Розчинність Sn в бінарній сполуці $HoFe_2$ (структурний тип $MgCu_2$) сягає до 5 ат. %.

Ключові слова: інтерметаліди; станіди; фазові діаграми; кристалічна структура; рентгенівська дифракція.